

Towards microfluidic reactors for in situ synchrotron infrared studies

I. P. Silverwood, N. Al-Rifai, E. Cao, D. J. Nelson, A. Chutia, P. P. Wells, S. P. Nolan, M. D. Frogley, G. Cinque, A. Gavriilidis, and C. R. A. Catlow

Citation: *Review of Scientific Instruments* **87**, 024101 (2016); doi: 10.1063/1.4941825

View online: <http://dx.doi.org/10.1063/1.4941825>

View Table of Contents: <http://scitation.aip.org/content/aip/journal/rsi/87/2?ver=pdfcov>

Published by the [AIP Publishing](#)

Articles you may be interested in

[Microfluidic reactors for visible-light photocatalytic water purification assisted with thermolysis](#)
Biomicrofluidics **8**, 054122 (2014); 10.1063/1.4899883

[A pulse chemisorption/reaction system for in situ and time-resolved DRIFTS studies of catalytic reactions on solid surfaces](#)

Rev. Sci. Instrum. **85**, 064103 (2014); 10.1063/1.4884795

[Alkene epoxidation with a polystyrene immobilised metal salen catalyst in a continuous-flow microfluidic reactor](#)

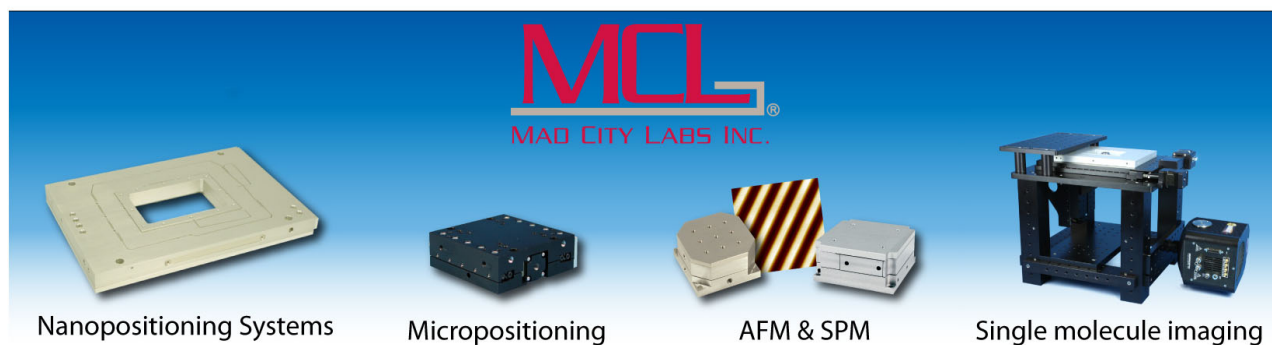
J. Appl. Phys. **105**, 102007 (2009); 10.1063/1.3116084

[Design and operating characteristics of a transient kinetic analysis catalysis reactor system employing in situ transmission Fourier transform infrared](#)

Rev. Sci. Instrum. **77**, 094104 (2006); 10.1063/1.2349602

[High pressure view-cell for simultaneous in situ infrared spectroscopy and phase behavior monitoring of multiphase chemical reactions](#)

Rev. Sci. Instrum. **74**, 4121 (2003); 10.1063/1.1597961



Towards microfluidic reactors for *in situ* synchrotron infrared studies

I. P. Silverwood,^{1,2,3,a)} N. Al-Rifai,⁴ E. Cao,⁴ D. J. Nelson,^{5,6} A. Chutia,^{1,2} P. P. Wells,^{1,2} S. P. Nolan,^{6,7} M. D. Frogley,⁸ G. Cinque,⁸ A. Gavrilidis,⁴ and C. R. A. Catlow^{1,2}

¹Department of Chemistry, University College London, London, WC1H 0AJ, United Kingdom

²UK Catalysis Hub, Research Complex at Harwell, Rutherford Appleton Laboratory, Harwell Oxford, OX11 0FA Didcot, United Kingdom

³ISIS Facility, STFC, Rutherford Appleton Laboratory, Harwell Oxford, OX11 0QX Didcot, United Kingdom

⁴Department of Chemical Engineering, University College London, London WC1E 7JE, United Kingdom

⁵Department of Pure & Applied Chemistry, University of Strathclyde, Glasgow G1 1XL, United Kingdom

⁶EaSTCHEM School of Chemistry, University of St Andrews, St Andrews KY16 9ST, United Kingdom

⁷Chemistry Department, King Saud University, Riyadh 11451, Saudi Arabia

⁸Diamond Light Source Ltd, Diamond House, Harwell Science and Innovation Campus, OX11 0DE Didcot, United Kingdom

(Received 21 October 2015; accepted 28 January 2016; published online 19 February 2016)

Anodically bonded etched silicon microfluidic devices that allow infrared spectroscopic measurement of solutions are reported. These extend spatially well-resolved *in situ* infrared measurement to higher temperatures and pressures than previously reported, making them useful for effectively time-resolved measurement of realistic catalytic processes. A data processing technique necessary for the mitigation of interference fringes caused by multiple reflections of the probe beam is also described. © 2016 AIP Publishing LLC. [<http://dx.doi.org/10.1063/1.4941825>]

I. INTRODUCTION

Catalytic reactions are industrially and financially important, with the value of goods and products dependent upon them estimated in 2009 as 15 trillion (US) dollars, which is equivalent to approximately one-third of the global GDP.¹ Improvement of catalytic processes is therefore key in increasing the sustainability of modern industry. To understand the nature of catalysis, measurement of reactions under conditions that do not perturb the reaction being studied, and as close as possible to relevant industrial conditions, is needed. This philosophy has come to be known as the “operando” method and has been growing in interest over the last decade.² One of the most illuminating tools for determining which species are present is infrared (IR) spectroscopy,³ which has been applied to *in situ* catalytic studies since the 1950s.^{4,5}

However, the apparatus used to study such systems often deviates from well-defined reaction conditions due to it being optimized for the spectroscopic demands of an instrument, rather than the requirements of the reaction.⁶

Another trend in reaction development is the application of microfluidics, which allows superior control over heat and mass transfer, and more efficient use of time and reagents.⁷ A wide range of materials has been used to manufacture devices in this growing field, including polydimethylsiloxane (PDMS),⁸ glass,⁹ encapsulated wax,¹⁰ CaF₂,¹¹ and even paper.¹² Of these materials, silicon is possibly the most enduring. Techniques developed from the manufacture of integrated circuits have led to exquisite control over the physical morphology of devices on the micro- and nano-scale. Anodic bonding of glass to silicon allows the production of reactors that have been used at elevated pressures and temperatures

(150 bars, 673 K)¹³ whilst presenting a chemically inert surface that will not affect the reaction of interest.

Combining infrared spectroscopy to monitor reactions *in situ* using silicon microfluidic reactors therefore allows an unprecedented amount of control over reaction parameters whilst decreasing compromises made in spectroscopic cell design. The high reflectivity of silicon in the infrared and opacity to visible light have so far limited its use for microfluidic devices in infrared studies. Measurement without spatial resolution has been reported by Floyd *et al.* in a fusion bonded reactor,¹⁴ and the high refractive index of silicon has been exploited in patterning reactors that incorporate an internal reflectance element to allow attenuated total reflectance (ATR) measurement.¹⁵

Spatially resolved investigation with IR to date has generally focussed on biological samples and flows of aqueous or relatively benign solvents that are compatible with other materials that allow visible light transmission. The two fundamental problems in developing IR-compatible microfluidic devices are patterning channels, and sealing them with a material that is at least reasonably IR-transparent. Sampling through a thin PDMS device has been demonstrated,¹⁶ but this material has interfering IR absorbances and limits the temperatures that can be used. CaF₂ devices have been manufactured by chemical etching and sealing with photoresist, which again imposes a relatively low temperature limit, and also prevents spectroscopy below 1000 cm⁻¹.¹¹ Paraffin wax channels have been printed directly onto optical elements and imaged using focal plane array (FPA) detectors.^{10,17} Microfluidic channels open to the atmosphere have also been used.¹⁸ None of these approaches can achieve the temperatures, pressures, and chemical resistance needed to study many catalytic reactions, and alternative sealing methods are of interest. The gold standard in this scenario is fusion bonding, where atomically flat Si surfaces are contacted and then annealed at 1000 °C.

^{a)}Author to whom correspondence should be addressed. Electronic mail: ian.silverwood@stfc.ac.uk

This approach has been demonstrated by Tan *et al.* to achieve limited spatial resolution, by using a FPA detector in transmission geometry to study CO oxidation over a Pt/SiO₂ catalyst.¹⁹ This bonding process is, however, highly demanding, and a more forgiving process that allows easier manufacture may increase adoption of the technique. Anodically bonded glass-silicon devices may therefore represent the best opportunity for robust, spectroscopically relevant reactors as the process forms a reliable, hermetic seal providing simple and rapid reactor manufacture whilst maintaining integrity at elevated temperature and pressure.

To obtain the most meaningful spectra from such reactors, high spatial resolution when acquiring spectra is needed to distinguish composition changes along the reactor length. Using reactors of known dimensions and specifying flow rates, position in the reaction channel with flow rate can also be used to obtain kinetic information. Higher spatial resolution therefore equates to higher time resolution when working in this regime. Diffraction limited spatial resolution (a few μm) may be achieved with infrared spectroscopy by using an infrared microscope system and a synchrotron light source. Using a computer controlled translation stage, it is possible to map a sample, obtaining spectra from an arbitrary number of separate points and combine them into a “chemical image” that represents composition as a function of position. This approach has been demonstrated with a simple reactor in a recent publication by Gross *et al.*²⁰ and is well developed in Raman microspectroscopy. This approach is more flexible than that offered by ATR, which can offer high spatial resolution,²¹ but only across the limited area of the ATR crystal (2 mm² for typical imaging ATR). ATR is further complicated by the fact that the penetration depth of light into the sample is small, and both wavelength and material dependent.

This work reports the manufacture and application of silicon microfluidic devices that provide IR transparency, good heat transfer properties, and non-turbulent flow to investigate a model catalytic reaction using microimaging FTIR with a synchrotron source.

II. EXPERIMENTAL

A. Device manufacture

Channels were patterned onto double-polished 4 in. diameter (1 0 0) silicon wafers of 525 μm thickness (Pi-Kem Ltd). A thick layer of photoresist (Rohm and Haas SPR-220-7) was applied by spin coating, baked, and exposed with a Quintel Q4000-6 mask aligner. This was etched to 30 μm with deep reactive ion etching (STS ICP DRIE) and the wafers cut using an automated saw (Disco DAD 3230). Etch depth was checked using a DektakXT surface profiler. The remaining photoresist was removed using acetone, before immersion in hot piranha solution (290 K, 20 min), rinsing in deionized water and drying in a nitrogen stream. Corning 7740 glass pieces of matching dimension that had been drilled for liquid connection and polished were obtained from Newcastle Optical Engineering. Au was sputter coated onto these through a shadow mask hand-cut from acetate sheet to provide reflective bands that crossed the flow channels. The silicon and glass pieces were hermetically

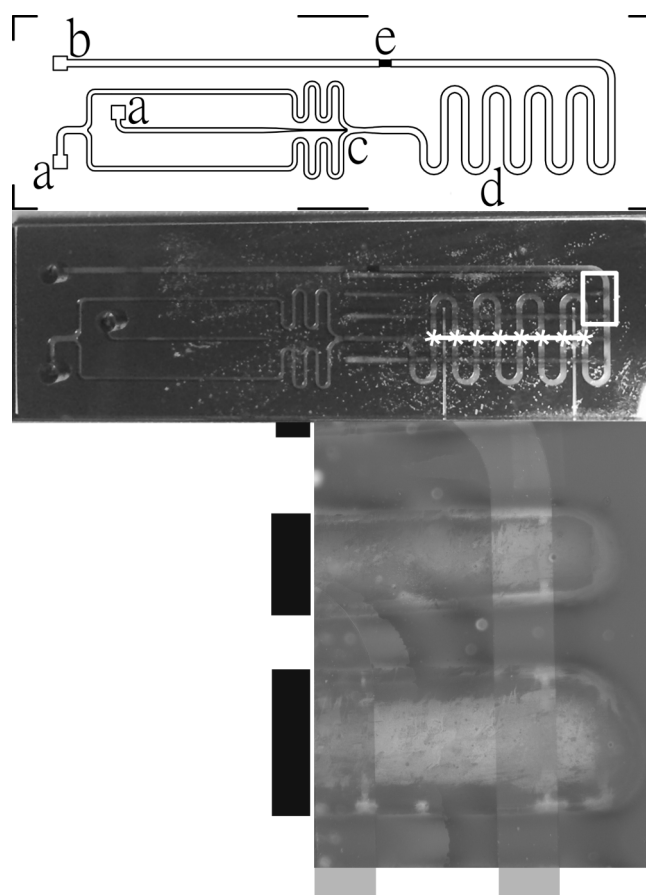


FIG. 1. Microfluidic device in (top) outline (centre) photograph and (bottom) detail. The area magnified is indicated in the photograph by the rectangular outline. Locations indicated on the device are (a) inlets, (b) outlet, (c) mixing point, (d) serpentine reaction path, and (e) filter/frit. To guide the eye in the magnified image, indicating areas aligned with the vertical reaction channels, and horizontal gold reflector pathways. The spectra in Figure 5 were collected at every point where the line on the photograph crosses the flow channel, with point 1 nearest the inlet (on the left) as shown.

sealed by anodic bonding at ~ 700 K and 800 V using a modified hotplate and high voltage power supply. Annotated photographs of the reactor are shown in Figure 1. The cells were mounted in a custom made heated microscope stage manufactured by Linkam as previously described elsewhere.²² Sealing was achieved by compressing the device against o-rings contained in the mount. Fluid supply to the channels was via 1/16 in. OD tubing of PTFE (polytetrafluoroethane), stainless steel, and PEEK (Polyether ether ketone) and controlled using two syringe pumps (World Precision Instruments Aladdin).

B. Infrared spectroscopy

Infrared data were recorded using the Multimode InfraRed Imaging And Microscopy (MIRIAM) beamline at B22 at the Diamond Light Source. The spectrometer was a Bruker Vertex 80 V using a Hyperion 3000 microscope with computerized xy stage. Spectra were collected in transfection mode with a 36 \times objective, and a single channel broadband MCT detector. *Ex situ* measurements were performed using a Nicolet IS10 with Smart ITR accessory using a toluene background. This had a diamond ATR crystal, Globar source, and DTGS detector. All spectra are presented in units of absorbance.

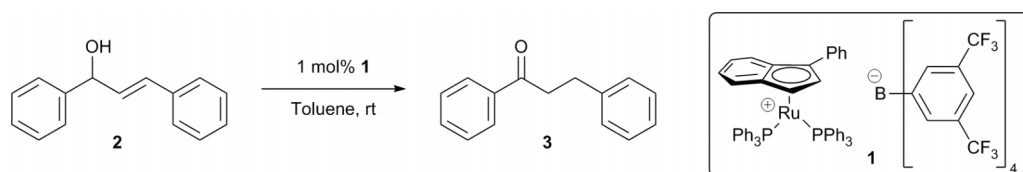


FIG. 2. Model reaction used for the study.

C. Materials and synthesis

The reaction studied was the catalytic isomerisation of allylic alcohols to ketones, which is synthetically useful and atom economical.²³ The catalyst in this case was a cationic ruthenium complex (**1**)²⁴ which has been shown to catalyse the isomerisation reaction at low (<1 mol. %) loadings;²⁵ the reaction is entirely homogeneous and does not require any additional reagents, which makes the reaction operationally simple and reduces the risk of blocking the small channels in the device. For this study, readily available 1,3-diphenylprop-2-ene-1-ol (**2**) was used as the substrate (Figure 2). The disappearance of the key OH stretch and growth of the CO stretch in the product (1,3-diphenylpropan-1-one, (**3**)) allow this reaction to be monitored.

The catalyst complex was prepared according to the published procedure,²⁴ and its purity was confirmed by elemental analysis. Substrate (**2**) was purchased from Sigma-Aldrich and used as supplied. While the catalyst is stable to air and atmospheric moisture in the solid state, it is much more air-sensitive when in solution; solutions of the catalyst and the substrate were therefore prepared in anhydrous, degassed toluene and loaded into syringes immediately before the experiment, using standard Schlenk techniques.

III. RESULTS

Measurements using the microscope optics with the internal Globar of the spectrometer were attempted before use of synchrotron light. It was found that reasonable spectra could not be achieved due to the high reflectivity of the silicon, and the required deep focus of the light. To obtain reasonable light flux, a large aperture was needed, which prevented a tight beam focus. With this arrangement, reflections from the top surface of the microchannel device were not rejected and this stray light dominated the obtained spectra and prevented optimisation of the focus at the channel depth. The high brightness and tighter focus of synchrotron IR allows a smaller confocal aperture to be used which restricts the depth of field. Rejection of light from the top surface allowed spectra to be collected from within the device. With the 30 μm channel depth used, it was not possible to restrict the aperture sufficiently to focus solely on the bottom face of the channel and interference patterns were observed between reflected light from the top and bottom of the channel, i.e., the internal silicon and gold/glass faces, respectively. The frequency of these fringes was used to confirm the channel depth and their magnitude provided a strong contrast between the void of the channel and the presence of silicon. This allowed easy location of the channels for subsequent measurement. Figure 3 displays a map of the

mixing point ((c) in Figure 1) obtained at 8 cm^{-1} resolution with 128 scans co-added at each point. Measurement points were spaced by approximately 50 μm and intensity is displayed as the integrated absorbance across the entire spectral range.

When the channels were filled with solvent, the contrast between channel and silicon became less apparent, which was attributed to high solvent absorbance and decreased reflection caused by the closer refractive index of toluene to silicon. Optimisation was carried out by focussing the optics to give maximum solvent absorbance relative to total signal intensity.

To demonstrate reaction monitoring, data were acquired at points along the serpentine path, as shown in Figure 1. This was necessary to account for spatial variations in the reflectivity of the cell. For each measurement, a background was collected with 40 $\mu\text{l/h}$ total flow solvent, before collecting the sample scan with 20 $\mu\text{l/h}$ alcohol and 20 $\mu\text{l/h}$ catalyst solutions, which provided a residence time of approximately 2 min and data were collected after thorough purging. All background scans were recorded before changing the flow conditions. Reproducible positioning of the sample stage was therefore key to the measurement. Collection parameters were 4 cm^{-1} resolution, 1024 scans, 30 μm aperture, and 40 $^{\circ}\text{C}$.

An overview of the data treatment is shown in Figure 4. The oscillations in the single beam spectra, due to interference of the IR reflections from top and bottom of the channel

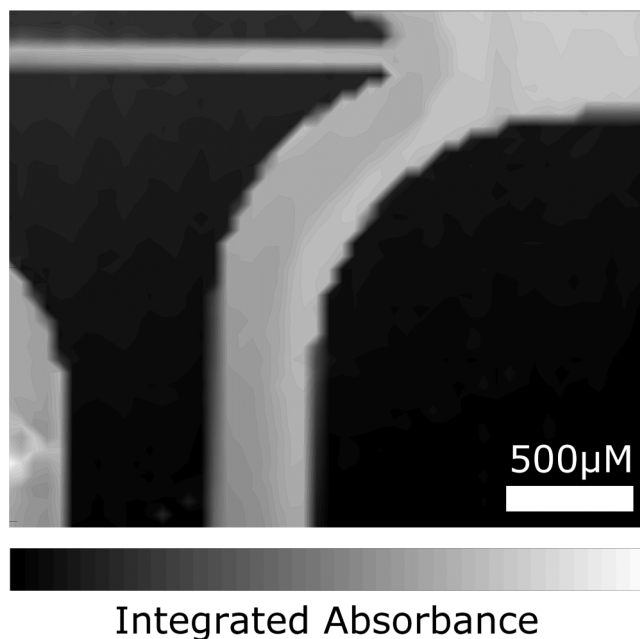


FIG. 3. IR absorbance map of mixing zone on chip (point (c) Figure 1).

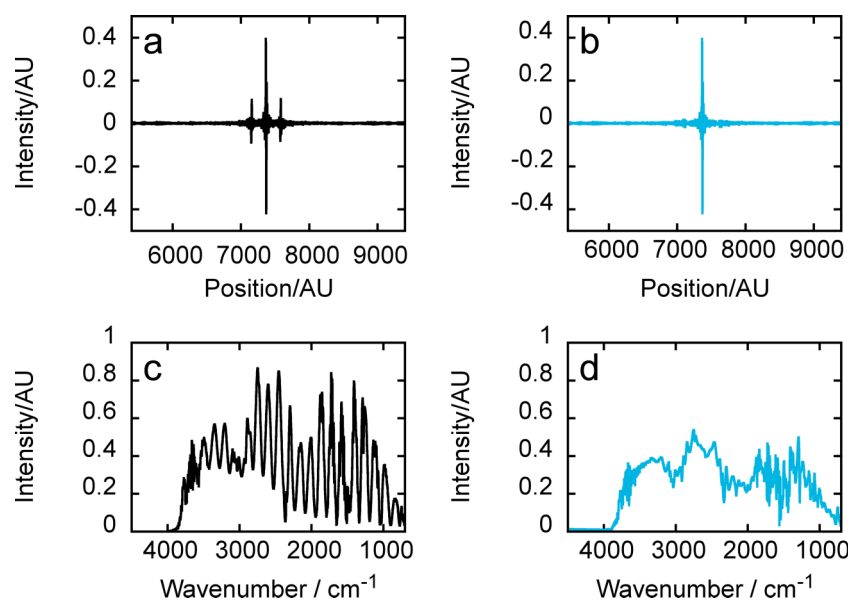


FIG. 4. Overview of data treatment showing interferograms before (a) and after (b) apodisation; single beam spectra obtained by Fourier transform of raw (c) and apodized (d) interferograms.

(Figure 4(c)), manifest in the interferogram (Figure 4(a)) as secondary bursts in intensity, also known as “ghost centre-bursts,” either side of the centre burst at zero path difference. There are numerous methods reported in the literature to ameliorate this effect.^{26–28} A semi-automated correction procedure was written using Microsoft Excel, which identified the maxima of the secondary bursts and generated an apodisation function with two Gaussian curves centred at these positions. An example calculation and data set is provided as electronic supplementary material.²⁹ After apodisation, the modified interferogram (Figure 4(b)) was Fourier transformed to give the single beam spectra (Figure 4(d)) which was then treated conventionally. The apodisation process was carried out independently for background and sample spectra. The spectra obtained after data processing are presented in Figure 5, with reference spectra of component solutions and batch reaction recorded using *ex situ* ATR after 2 min. The data in the enumerated channels show weak oscillations in the baseline due to an artefact which remains after data correction, but overall the spectra appear to be of reasonable quality. It should be remembered that solvent absorbances dominate and features in the ranges 1635–1370 and 1115–1015 cm^{-1} may be masked due to high toluene absorption. Spectra 5–8 in Figure 5 show noise around 1500 cm^{-1} (b) that illustrates the miscancellation of the solvent signal. Measuring the spectrum of the alcohol in solution proved difficult due to this effect as its bands overlapped with solvent bands. The most diagnostic band for the alcohol, as demonstrated in the ATR spectra, was at 965 cm^{-1} , assigned to the unsaturated CH bending mode (f). As the ketone product shows a band at 974 cm^{-1} , and both appear broad there is some overlap between the spectra of these species. The strongest band in the ketone spectrum is the C=O stretch at 1688 cm^{-1} (a), and is clearly diagnostic of the product. The ATR of the reaction solution shows that the dominant features in the reaction solution belong to the catalyst, with the bands highlighted at 1354, 1278, and 1128 cm^{-1} (c)–(e) appearing strong. There is also

a weak ketone band at 1688 cm^{-1} (a) that illustrates only moderate reaction has occurred. This is in contrast to previous and subsequent measurement of the reaction, which has high conversion and selectivity, suggesting the catalyst batch used here was somehow defective. Due to competition for access to synchrotron beamtime, it was unfortunately not possible to repeat the experiment with another batch of catalyst.

In the data collected with the microfluidic device, there is little evidence for the alcohol reactant or the ketone product, which may be due to incomplete mixing and low conversion. However, the bands corresponding to the catalyst are present and display variation with position, indicating that some reaction is occurring. With increasing distance along the reaction channel, the band at 1278 cm^{-1} (d) decreases in intensity, and

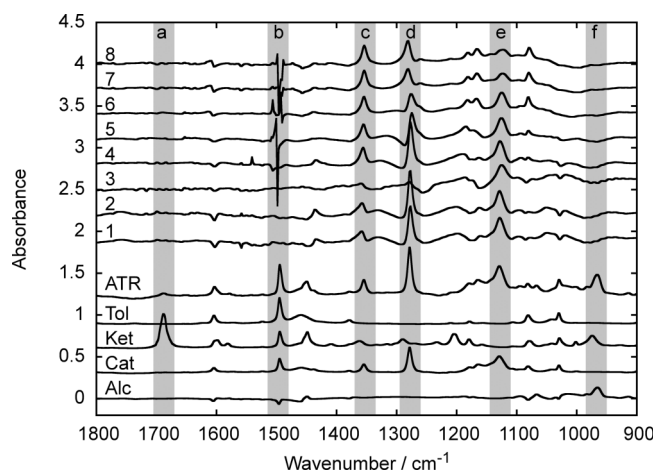


FIG. 5. Infrared absorbance spectra collected at increasing distance along the reaction channel (channel 1 nearest inlet), with ATR reference spectra of the reaction mix (ATR), ketone (Ket), catalyst (Cat), and Alcohol (Alc). Spectrum of the toluene solvent (Tol) recorded using air background. Grey bands highlight major features referred to in text and cover ranges (a) 1705–1670, (b) 1515–1480, (c) 1370–1335, (d) 1295–1260, (e) 1145–1110, and (f) 985–950 cm^{-1} .

the 1354 band (c) increases. The 1128 band (e) becomes less defined, with features appearing on either side at 1182, 1166, and 1078 cm^{-1} . This reflects the changes seen in the ATR measurement after 2 min reaction and demonstrates the ability to collect spatially resolved, diagnostic spectra of chemicals undergoing rapid change when dissolved in highly absorbing solvents. Although the desired reaction was not observed, the IR data from the two measurements is consistent and demonstrates the utility of the microfluidic devices.

IV. DISCUSSION

Mapping of microfluidic devices that expand possible reaction conditions has been demonstrated with good spatial and spectroscopic resolution. The *ex situ* ATR spectroscopy shows low conversion of the alcohol after 2 min reaction, which is in contrast to previous measurements and suggests that there may have been issues with the integrity of the catalyst, possibly due to reaction with dissolved oxygen. Alternatively, there may be poor mixing or an initiation period at the start of the reaction, which would not have been observed during the synthetic experiments previously carried out due to their longer timeframe. The flow pattern chosen has not been optimized for the reaction studied, and there is the possibility that laminar flow is occurring after the mixing point of the two flows. However, the observable changes along the flow path relate to those seen with ATR, providing evidence of reaction progress. Reaction will occur at the interface in laminar flow, and since the IR beam sampled the reactor with an approximate cross section of $30 \times 30 \mu\text{m}$, the measurement will represent an average over a portion of the channel width. As data collection took a few minutes at each point, it will also be time-averaged to some degree and small fluctuations removed. The rate of mixing is key to understanding of chemical reactions and whilst not investigated here, controlling this parameter through reactor design is of great interest. Use of infrared spectroscopy in this mode to quantify the changes in comparable reactors should be able to provide insight in future chip design. The spectroscopy has shown that it is possible to observe catalyst in solution, and with a more robust chemical system it should be possible to fully observe catalytic reactions. Although substantial data processing is needed to eliminate interference, and may introduce minor artefacts, the spectra appear consistent and this could be automated more fully in the future. Adaptation of the design to improve these problems may be possible, using anti-reflection coatings, non-parallel surfaces, or decreasing depth of field.

V. CONCLUSIONS

The application of glass-silicon reactors expands the reaction environment to allow operation at more relevant process conditions and there are encouraging opportunities for further development of this technique. The rapid and flex-

ible manufacturing process allows the production of reactors tailored to the chemistry and spectroscopic characteristics of the system of interest. Previous compromises in reactor design can be eliminated to provide future optimized *operando* measurement. Infrared spectroscopy is an ideal probe for many chemical systems, and through careful reactor design it may be coupled to a very broad range of reacting chemical and biological systems with high temporal and spatial resolution.

ACKNOWLEDGMENTS

UK Catalysis Hub is kindly thanked for resources and support provided via our membership of the UK Catalysis Hub Consortium and funded by EPSRC (portfolio Grant Nos. EP/K014706/1, EP/K014668/1, EP/K014854/1, and EP/K014714/1). We thank Diamond Light Source for access to beamline B22 (Proposal No. SM8962-1) that contributed to the results presented here.

- ¹C. Adams, *Top. Catal.* **52**, 924 (2009).
- ²C. O. Areal, B. M. Weckhuysen, and A. Zecchina, *Phys. Chem. Chem. Phys.* **14**, 2125 (2012).
- ³F. Zaera, *Chem. Soc. Rev.* **43**, 7624 (2014).
- ⁴R. P. Eischens, W. A. Pliskin, and S. A. Francis, *J. Chem. Phys.* **22**, 1786 (1954).
- ⁵J. E. Mapes and R. P. Eischens, *J. Phys. Chem.* **58**, 1059 (1954).
- ⁶F. C. Meunier, A. Goguet, S. Shekhtman, D. Rooney, and H. Daly, *Appl. Catal. A* **340**, 196 (2008).
- ⁷A. Gavrilidis, P. Angeli, E. Cao, K. K. Yeong, and Y. S. S. Wan, *Chem. Eng. Res. Des.* **80**, 3 (2002).
- ⁸J. Friend and L. Yeo, *Biomicrofluidics* **4**, 026502 (2010).
- ⁹J. Kotowski, V. Navrátil, Z. Slouka, and D. Šnita, *Microelectron. Eng.* **110**, 441 (2013).
- ¹⁰A. Chan, X. Niu, A. de Mello, and S. Kazarian, *Lab Chip* **10**, 2170 (2010).
- ¹¹T. Pan, R. T. Kelly, M. C. Asplund, and A. T. Woolley, *J. Chromatogr. A* **1027**, 231 (2004).
- ¹²A. K. Yetisen, M. S. Akram, and C. R. Lowe, *Lab Chip* **13**, 2210 (2013).
- ¹³N. Al-Rifai, E. Cao, V. Dua, and A. Gavrilidis, *Curr. Opin. Chem. Eng.* **2**, 338 (2013).
- ¹⁴T. M. Floyd, M. A. Schmidt, and K. F. Jensen, *Ind. Eng. Chem. Res.* **44**, 2351 (2005).
- ¹⁵X. Liu, B. Ünal, and K. Jensen, *Catal. Sci. Technol.* **2**, 2134 (2012).
- ¹⁶M. V. Barich and A. T. Krummel, *Anal. Chem.* **85**, 10000 (2013).
- ¹⁷A. Chan and S. Kazarian, *Anal. Chem.* **84**, 4052 (2012).
- ¹⁸H.-Y. Holman, R. Miles, Z. Hao, E. Wozel, M. Anderson, and H. Yang, *Anal. Chem.* **81**, 8564 (2009).
- ¹⁹C. K. C. Tan, W. N. Delgass, and C. D. Baertsch, *Appl. Catal. B* **93**, 66 (2009).
- ²⁰E. Gross, X.-Z. Shu, S. Alayoglu, H. A. Bechtel, M. C. Martin, F. D. Toste, and G. A. Somorjai, *J. Am. Chem. Soc.* **136**, 3624 (2014).
- ²¹K. L. A. Chan, S. G. Kazarian, A. Mavraki, and D. R. Williams, *Appl. Spectrosc.* **59**, 149 (2005).
- ²²E. Cao, M. Sankar, S. Firth, K. Lam, D. Bethell, D. Knight, G. Hutchings, P. McMillan, and A. Gavrilidis, *Chem. Eng. J.* **167**, 734 (2011).
- ²³R. Uma, C. Crévisy, and R. Grée, *Chem. Rev.* **103**, 27 (2003).
- ²⁴S. Manzini, D. J. Nelson, and S. P. Nolan, *ChemCatChem* **5**, 2848 (2013).
- ²⁵S. Manzini, A. Poater, D. J. Nelson, L. Cavallo, and S. P. Nolan, *Chem. Sci.* **5**, 180 (2014).
- ²⁶M. F. Faggin and M. A. Hines, *Rev. Sci. Instrum.* **75**, 4547 (2004).
- ²⁷F. R. S. Clark and D. J. Moffatt, *Appl. Spectrosc.* **32**, 547 (1978).
- ²⁸T. Hirschfeld and A. W. Mantz, *Appl. Spectrosc.* **30**, 552 (1976).
- ²⁹See supplementary material at <http://dx.doi.org/10.1063/1.4941825> for fringe elimination procedure.